A New 1D-CNN Paradigm for Onset Detection of Absence Seizures in Children

Maxime Yochum[1], Amar Kachenoura[1], Matthieu Aud'hui[1], Fabrice Wendling[1], Anna Kaminska[2], Rima Nabbout[2], Mathieu Kuchenbuch[3], Pascal Benquet[1]

[1] University of Rennes
INSERM, LTSI-U1099
35000 Rennes, France
maxime.yochum@univ-rennes.fr
amar.kachenoura@univ-rennes.fr
matthieu.audhui@univ-rennes.fr
fabrice.wendling@inserm.fr
pascal.benquet@univ-rennes.fr

[2] Hopital Necker Enfants Malades,
Institute Imagine INSERM 1163,
Universite de Paris, Paris, France.
anna.kamins@aphp.fr
rima.nabbout@aphp.fr

[3] Pediatric and Genetic Department
CHU , Nancy, France
m.kuchenbuch@chru-nancy.fr

***Abstract*—This study presents a One-Dimensional Convolutional Neural Network (1D-CNN)-based algorithm for the early detection of childhood absence seizures in ElectroEncephaloGraphy (EEG) traces. This detection aims to enable timely sensory interventions, such as acoustic or visual stimulation, to potentially abort seizures. The algorithm was evaluated using a clinical setting with full EEG data and a reduced number of electrodes version of the data to show its suitability in a normal child environment. On the clinical EEG database of 117 patients, the model achieved promising results, including a Sensitivity of 0.859, Precision of 0.819, F1-score of 0.837, and a mean detection delay of 0.522 seconds. The performance remained satisfactory when using fewer electrodes, with a Sensitivity of 0.837, Precision of 0.808, F1-score of 0.820, and similar detection delays. These results demonstrate the method's robustness and feasibility for clinical applications, as well as its potential to be embedded in wearable devices for continuous, real-time seizure monitoring and intervention in children with absence epilepsy.**

Keywords-Surface EEG; Childhood Absence Epilepsy; Onset Detection; 1D-CNN.

I. INTRODUCTION

Typical absence seizures are characterized by brief and sudden lapses in consciousness and an absence of voluntary movements. Typically, they are associated with specific patterns of generalized spike-wave discharges observed in EEG recordings [1]. Childhood Absence Epilepsy (CAE) affects between 6.3 to 8.0 children per 100 000 annually [2] and accounts for 18% of all cases of epilepsy in school-aged children. Absence seizures, if untreated, can occur frequently throughout the day, sometimes up to 200 episodes daily [3]. Children with CAE generally follow a normal developmental path. Nevertheless, approximately 30% of them experience learning difficulties and Attention Deficit Hyperactivity Disorder (ADHD).

The diagnosis of CAE often involves a physical exam with an EEG routine during voluntary hyperventilation. On EEG, seizures are commonly associated with 3-4 Hz generalized spike-wave patterns, but variations in speed, symmetry, and the presence of polyspikes may also be observed. The treatment of absence seizures typically involves antiepileptic drugs, although there is a notable drug resistance rate of approximately 30% [4]. As an alternative to drug therapy, sensory or electrical stimulation techniques have shown promise in interrupting seizures [5], [6]. Research on rodent models has demonstrated that auditory stimuli, such as a 2 kHz tone, during the first few seconds of the seizure can stop around 52% of absence seizures [6]. In humans[7], simple acoustic stimuli delivered during the first 3 seconds of the seizure can inhibit the episode with a success rate of 57%. Thus, detecting the onset of seizures as early as possible is crucial for effectively applying these kinds of stimulation techniques. Numerous studies for absence seizure detection from surface EEG signals have been reported during the last decades [8]–[12]. Surprisingly, none of these approaches have focused on early detection, i.e., identifying seizure within one second of its onset, which is crucial for applying external stimulation to abort seizures as the stimulation must occur within the first seconds of the seizure [7]. To address this gap, the paper proposes a new Deep Learning-based (DL) approach designed for early detection of absence seizures from raw EEG data. The method uses a learned 1D-CNN model to identify seizure onset within short sliding windows of EEG data in real-time, making it suitable for integration into wearable devices. This approach improves accuracy by analyzing data across multiple EEG channels. Additional constraints on the consecutive detection of the onset of seizures and the number of channels, where the seizure is detected, are also proposed to minimize the False Detection Rate (FDR), ensuring robustness of the pipeline in real-world applications.

This communication is organized as follows: the dataset, the CNN-based model and the evaluation criteria are presented in Section II. The obtained results are reported in Section III. Discussion, conclusions and perspectives are given in Section IV.

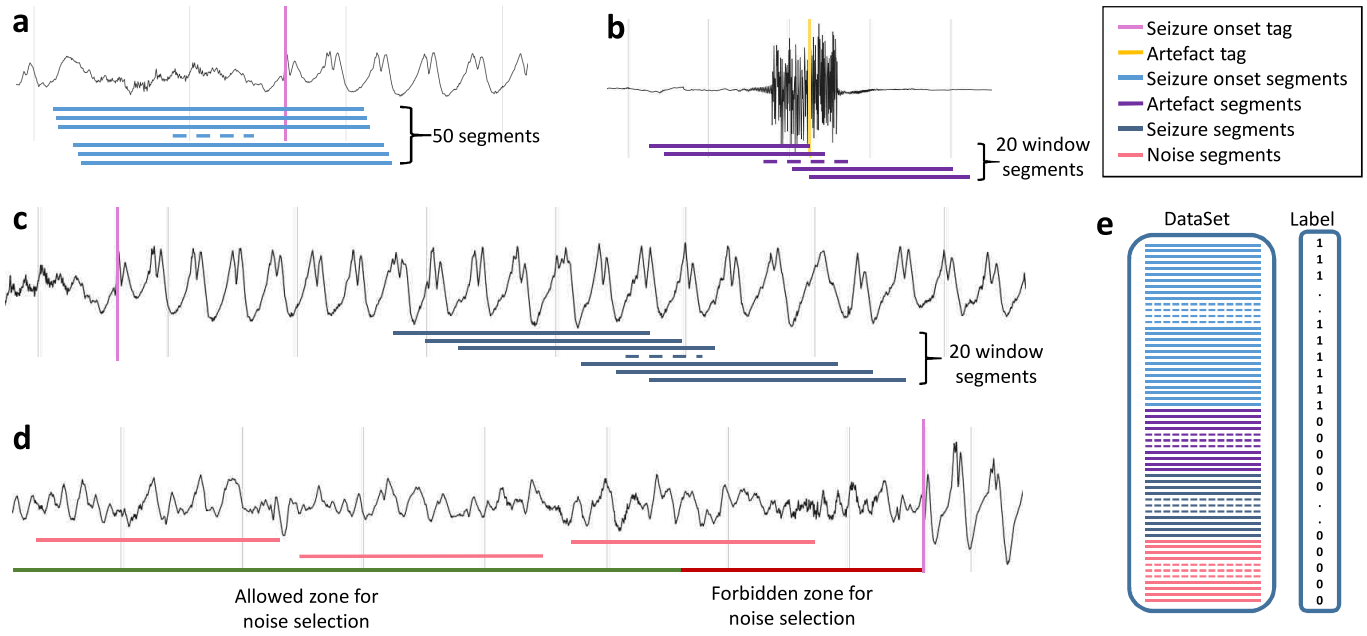

Figure 1. a. Selection of 50 segments for the seizure onset. The first segment is selected so the expert onset tag is located at the 384^{th} sample. The other segments are shifted from the first one from 1 to 49 samples. b. 20 segments were picked from -2 to 2s around the artifact tag (yellow position). c. 20 seizure segments were picked starting from 2s to 4s after the seizure onset tag. d. Noise segments were picked where seizure onset tags were absent within 2s from the starting noise segment.

II. Material and Method

The annotated dataset, the data-driven model design and the evaluation metrics are described in this section.

A. EEG recordings

In this study, EEG signals issued from 117 children (53 females and 64 males) diagnosed with CAE were used for evaluating the proposed pipeline. The dataset was acquired between 2013 and 2019, following the guidelines outlined in the French recommendations for EEG procedures in children [13] under the study protocol IRB:IORG0010044. The children were between 4 and 11 years old, and the recordings were conducted at two medical centers: Saint-Brieuc Hospital and Necker-Enfants Malades Hospital. The study strictly excluded children with intellectual disabilities or relevant neurological abnormalities based on the new classification of epileptic syndromes. EEG signals were acquired using the Deltamed Natus system at 256 Hz sampling frequency, with recordings lasting at least 20 minutes. The number of EEG electrodes varied across recordings, depending on the age of the patients, with 11, 16, or 19 electrodes used. Following the 10/20 international system, these recordings resulted in a total duration of 2.75 days of EEG data, or 49.9 days when measured across one EEG channel. As the signals are z-score normalized for each EEG trace, no magnitude scale was given in all figures.

B. EEGs annotation

It is well-known that the ground truth is mandatory for the performance evaluation of machine learning methods. In our study, clinical experts visually annotated the seizure onset times to create a ground truth for training the model and validate the detection of the proposed procedure. The experts used dedicated software to mark seizure onset times across each EEG channel in a recording. To ensure consistency, two strict criteria were applied for selecting seizure events: (1) at least four consecutive spike-wave occurrences had to be visually detected, and (2) spike-waves had to be visible on at least half of the EEG channels. This ensured that only generalized seizures were included in the analysis, leading to 827 early seizure onset positions used for training and testing.

C. Training data set building strategy

An adequate design of the training data set is important to construct an efficient and stable DL model. Thus, to address the specific task of early detection of absence seizure onset, the training set was built by dividing the EEG data into two sets of 2-second segments: the first one contains seizure onset segments and the second one encompasses non-seizure onset segments. More precisely, as depicted in Figure 1-a, the seizure onset set was constructed, by extracting 50 segments from each onset expert tags. These segments were designed to capture temporal information around the seizure onset by varying their relative position to the expert onset. This allows the model to learn the dynamic transition from background EEG to seizure activity. The seizure onset expert tags, positioned around 1.5 seconds of the window, ensure the presence of 1.5 to 2 spike waves at the end of the seizure onset segments which contributed to a comprehensive analysis of onset seizure events. Regarding the non-seizure onset set, it includes three subcategories of EEG signals: background

EEG, physiological and non-physiological artifacts, and fully developed seizure segments (Figure 1-b). Background EEG was randomly selected to represent a broad spectrum of normal brain activity (Figure 1-d). Artifact segments, such as those caused by patient movements, eye movements, or amplifier disconnections, were included to avoid detecting them as false positives (Figure 1-b). In addition, fully developed seizure segments (Figure 1-c) were also added to ensure that the model could differentiate between the onset of a seizure and the more periodic, established spike-wave patterns of a full seizure.

D. DL-based model architecture

The proposed model is designed to analyze each EEG electrode independently. Analyzing each EEG channel independently ensures flexibility across different EEG systems and configurations, making it suitable for various clinical settings. The model consists of four 1D convolutional layers with progressively increasing numbers of filters (from 32 to 256), followed by average pooling layers, a flatten layer, and two fully connected layers. A dropout rate of 50% was applied to prevent overfitting, and the Rectified Linear Unit (ReLU) activation function was used throughout the network. The final output layer used a Softmax activation function to classify segments as either seizure onset or non-seizure onset. The training was optimized using the Adam algorithm, with a batch size of 128, 10 epochs, and a learning rate of 0.001.

E. Training, detection stages

To ensure the generalizability, robustness, and stability of the proposed DL-based method, the training stage involved constructing 12 bootstrap datasets, with 80% of patients allocated for training and 20% for testing. Importantly, the model was trained based on a non-patient-specific detection strategy. For each bootstrap, patients included in the training set were excluded from the testing set. During the detection phase (testing stage), for each tested patient, the trained model was applied on each EEG channel using a 2-second sliding window with a 1-sample shift. Segments were classified as Event of Interest (EoI) based on the output probability of the 1D-CNN exceeding a threshold T. However, the sliding window approach could lead to multiple detections of the same seizure onset, artificially exaggerating the FDR. To reduce this issue, a post-processing step was introduced. It is based on two thresholds: i) if the percentage of the number of positive detections within the N consecutive 2 s time windows is higher than a threshold Pw%, then the final sample of the last window is qualified to be a seizure onset position, and ii) the end of this last window is definitively tagged as a seizure onset if it was simultaneously detected on a minimum percentage of EEG channels (denoted as Pch%).

F. Evaluation metrics

In this study, the Sensitivity (S), Precision (P), F1-score and FDR per Hour (FDR/H) metrics [14] are used to evaluate the seizure onset detection performance of the proposed pipeline. The limit for the detection was fixed to 2 seconds from an expert tag: if a detection of our algorithm is out of this ±2s bound, it is considered as a False Positive (FP).

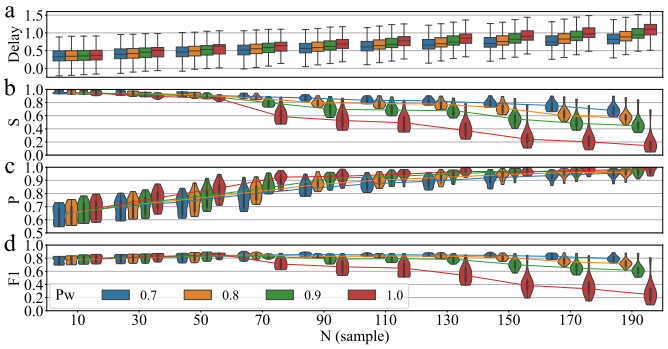

Figure 2. All plots x-axis represent the length (in sample) of the consecutive window use along with the Pw threshold, In all plots, each color used represents a Pw value (blue: Pw=70%; orange: Pw=80%; green: Pw=90%; red: Pw=100%). a. Boxplot of the delays of the algorithm detection with respect to the expert tags. b-d. violin plot of the Sensitivity (b), Precision (c) and F1-score (d).

III. RESULTS

The first experiment was conducted to determine a good compromise between the number N of the consecutive 2 s time windows and the threshold Pw. Regarding the Pch (minimum number of channels where the onset was simultaneously detected), it was fixed to 50% in the sequel. Figures 2 (a), (b), (c) and (d) display the delays, in seconds, of the algorithm detections relative to the expert annotations, S, P and F1-score, respectively, for all tested patients (across the 12 bootstraps). Four values of Pw=70% (blue), 80%(orange), 90% (green),100% (red) were tested, where the number N was varied from 10 to 190 with a step of 20. It can be seen from Figure 2 (a) that as N increases, the detection delay becomes more pronounced, regardless Pw. Figure 2 (b) shows that Sensitivity decreases significantly for $N > 50$, while Precision increases with increasing N, indicating a reduction in false detection. Interestingly, the best F1-score, defined as the harmonic average of the Sensitivity and the Precision, was obtained for $N = 50$ and Pw=80%, with a satisfactory detection delay around 0.5 s. Figure 3 focuses on the results obtained for Pw=80%, $N = 50$, and Pch=50% across all bootstraps. The average F1-score across all bootstraps was 0.837 ± 0.032, reflecting the model's effectiveness in detecting seizure onsets. Sensitivity and Precision were also well-balanced, with averages of 0.859 ± 0.030 and 0.819 ± 0.064, respectively, while the FDR/H remained low at 1.78 ±0.49. Furthermore, the delay between the detected seizure onsets and expert annotations was minimal, with an average delay of 0.522 seconds and a maximum delay of 1.5 seconds, as shown in Figure 3 (b). These results confirm the model's ability for very early seizure detection. Additionally, the proposed pipeline demonstrated robustness across different training and testing sets, since the standard deviations were low, whatever the analyzed metric.

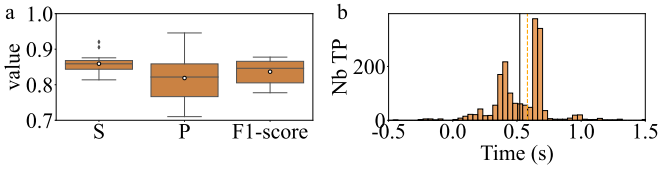

Figure 3. a: Sensitivity (S), Precision (P) and F1-score computed from the best F1 score of each Bootstrap (in blue) and for a unique triplet (in orange), means are shown with white circles. Histogram of delays measured between the expert annotation and the detected seizure onset moments by our algorithm for separate bootstrap optimization (b) and overall bootstrap triplet (c).

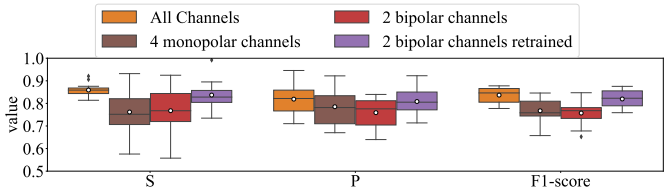

Figure 4. Sensitivity (S), Precision (P) and F1-score computed from the best F1 score for an overall triplet in four different cases: All channels (in orange), 4 monopolar channels (in green), 2 bipolar channels (in red), 2 bipolar channels with a retrained DL model (in purple). Medians are shown with black lines and means are shown with white circles

The second experiment deals with the configuration of the wearable device, where we can only expect that four electrodes will be available. Thus, we evaluated our detector only with Fp1, Fp2, T3 and T4 electrodes. The choice of two prefrontal electrodes and two temporal electrodes was driven by the fact that they could be hidden in the temples of glasses. More precisely, the model used previously was applied in two different montages: i) on 4 monopolar EEG channels (brown in Figure 4), and ii) on two bipolar channels Fp1-T3 and Fp2-T4 (red in Figure 4). Bipolar montages are known to be less susceptible to artifacts and commonly used for clinical EEG recordings. The impaired statistics using a reduced number of EEG channels are presented in Figure 4. We observed that the optimal F1-scores and the related sensitivities and precisions decrease for both montages compared to the use of all electrodes. Logically, the number of FDR/H increased from 1.783 for all electrodes to 3.071 and 3.060 for four monopolar and two bipolar electrodes, respectively.

To enhance the applicability of the model to bipolar channels, we also evaluate a new model that was specifically trained only on bipolar channels FP1-T3 and FP2-T4. As expected, this adjustment led to a significant improvement in results, although it does not exactly reach the performance achieved using all EEG channels (purple vs orange boxplots in Figure 4). With respect to the Performances of the initial model applied on bipolar montage (red boxplots), the Sensitivity, Precision and F1-score were increased from 0.78 to 0. 837 (±0. 064), 0.771 to 0. 808(±0. 063), and 0.796 to 0. 820 (±0. 040), respectively. In addition, the FDR/H was improved from 3.06 to 2.03. Regarding the delays of the detection of the seizure onset, the mean delay was almost not impacted (0.460 s).

IV. Discussion an conclusion

The proposed study is based on existing research, which demonstrates that absence seizures can be inhibited if external sensory stimulation is applied early in the seizure onset. Detection of the onset of the absence seizure as early as possible is mandatory to abort seizure progression, as delayed stimulation becomes ineffective once the seizure is fully established. Although several studies have been dedicated to the automated detection of absence seizures, no technique has yet been designed for early seizure onset detection (less than one second from the onset). Thus, this study introduces a new 1D-CNN-based pipeline for the early detection of absence seizures in children. Furthermore, the pipeline did not need heavy preprocessing and can be implemented in wearable devices. The 1D-CNN was favored over other models, such as Long Short Term Memory (LSTM) and Temporal Convolutional Network (TCN), due to its simplicity, ease of parallelization, and performance efficiency in handling EEG data. For instance, the computational time for processing data from a 15-electrodes is only about 0.4 ms. Obtained results, on a large real database, show that the model is very efficient in detecting the onset of seizures in children, with a Sensitivity of 0.859, Precision of 0.819, and F1-score of 0.837, alongside a time delay of just 0.522 seconds from the expert annotations. Importantly, even with a reduced set of electrodes (two bipolar channels), the method maintained good performance, which indicates that the algorithm is well-suited for portable devices. An adjustment of some parameters in the postprocessing step can also provide a possibility for a tradeoff between FDR/H and the maximal delay of detection allowed by a physicist to abort seizures.

The study acknowledges certain limitations, including the challenge of dealing with false detection due to short spike trains, which clinicians do not consider as seizures. In addition, more intensive clinical or animal studies are necessary to determine the optimal window length for effective intervention. The exploited EEG data were collected in controlled environments, and future work should focus on validating the robustness of the proposed pipeline in more variable settings, particularly in wearable devices.

Acknowledgment

This study has been funded by the Institut des Neurosciences Cliniques de Rennes (INCR, www.incr.fr), as part of the PREDILEPSY Project, and the Agence nationale de la recherche (ANR) Recherche Hospitalo-Universitaire en santé (RHU) through the innov4-epik project.

References

[1] V. Crunelli *et al.*, “Clinical and experimental insight into pathophysiology, comorbidity and therapy of absence seizures,” *Brain*, vol. 143, no. 8, pp. 2341–2368, 2020.

[2] E. Hirsch *et al.*, “Ilae definition of the idiopathic generalized epilepsy syndromes: Position statement by the ilae task force on nosology and definitions,” *Epilepsia*, vol. 63, no. 6, pp. 1475–1499, 2022.

[3] M. R. de Feo, O. Mecarelli, G. Ricci, and M. F. Rina, "The utility of ambulatory eeg monitoring in typical absence seizures," *Brain and Development*, vol. 13, no. 4, pp. 223–227, 1991.

[4] M. Koutroumanidis *et al.*, "The role of eeg in the diagnosis and classification of the epilepsy syndromes: A tool for clinical practice by the ilae neurophysiology task force (part 1)," *Epileptic Disorders*, vol. 19, no. 3, pp. 233–298, 2017.

[5] H. Blumenfeld, "Consciousness and epilepsy: Why are patients with absence seizures absent?" *Progress in brain research*, vol. 150, pp. 271–603, 2005.

[6] S. Saillet *et al.*, "Neural adaptation to responsive stimulation: A comparison of auditory and deep brain stimulation in a rat model of absence epilepsy," *Brain stimulation*, vol. 6, no. 3, pp. 241–247, 2013.

[7] P. Rajna and C. Lona, "Sensory stimulation for inhibition of epileptic seizures," *Epilepsia*, vol. 30, no. 2, pp. 168–174, 1989.

[8] J. Duun-Henriksen *et al.*, "Automatic detection of childhood absence epilepsy seizures: Toward a monitoring device," *Pediatric neurology*, vol. 46, no. 5, pp. 287–292, 2012.

[9] P. Glaba *et al.*, "Absence seizure detection algorithm for portable eeg devices," *Frontiers in Neurology*, vol. 12, p. 685 814, 2021.

[10] T. W. Kjaer, H. B. Sorensen, S. Groenborg, C. R. Pedersen, and J. Duun-Henriksen, "Detection of paroxysms in long-term, single-channel eeg-monitoring of patients with typical absence seizures," *IEEE journal of translational engineering in health and medicine*, vol. 5, pp. 1–8, 2017.

[11] L. Swinnen *et al.*, "Accurate detection of typical absence seizures in adults and children using a two-channel electroencephalographic wearable behind the ears," *Epilepsia*, vol. 62, no. 11, pp. 2741–2752, 2021.

[12] C. Chatzichristos *et al.*, "Multimodal detection of typical absence seizures in home environment with wearable electrodes," *Frontiers in Signal Processing*, vol. 2, p. 1 014 700, 2022.

[13] A. Kaminska, F. Cheliout-Heraut, M. Eisermann, A. T. de Villepin, and M. Lamblin, "Eeg in children, in the laboratory or at the patient's bedside," *Neurophysiologie Clinique/Clinical Neurophysiology*, vol. 45, no. 1, pp. 65–74, 2015.

[14] M. Sokolova, N. Japkowicz, and S. Szpakowicz, "Beyond accuracy, f-score and roc: A family of discriminant measures for performance evaluation," in *Australasian joint conference on artificial intelligence*, Springer, 2006, pp. 1015–1021.